



This discussion paper is/has been under review for the journal Geoscientific Model Development (GMD). Please refer to the corresponding final paper in GMD if available.

Non-singular spherical harmonic expressions of geomagnetic vector and gradient tensor fields in the local north-oriented reference frame

J. Du^{1,2,3,4}, C. Chen^{1,3}, V. Lesur², and L. Wang^{1,3,4}

¹Institute of Geophysics & Geomatics, China University of Geosciences, Wuhan 430074, China

²Helmholtz Centre Potsdam, GFZ German Research Centre for Geosciences, 14473 Telegrafenberg, Germany

³Hubei Subsurface Multi-scale Imaging Lab (SMIL), China University of Geosciences, Wuhan 430074, China

⁴State Key Laboratory of Geodesy and Earth's Dynamics, Chinese Academy of Sciences, Wuhan 430077, China

Received: 27 October 2014 – Accepted: 4 November 2014 – Published: 5 December 2014

Correspondence to: J. Du (jinsongdu.cug@gmail.com)

Published by Copernicus Publications on behalf of the European Geosciences Union.

[Title Page](#)

[Abstract](#)

[Introduction](#)

[Conclusions](#)

[References](#)

[Tables](#)

[Figures](#)

◀

▶

◀

▶

[Back](#)

[Close](#)

[Full Screen / Esc](#)

[Printer-friendly Version](#)

[Interactive Discussion](#)

Abstract

General expressions of magnetic vector (MV) and magnetic gradient tensor (MGT) in terms of the first- and second-order derivatives of spherical harmonics at different degrees and orders, are relatively complicated and singular at the poles. In this paper, 5 we derived alternative non-singular expressions for the MV, the MGT and also the higher-order partial derivatives of the magnetic field in local north-oriented reference frame. Using our newly derived formulae, the magnetic potential, vector and gradient tensor fields at an altitude of 300 km are calculated based on a global lithospheric magnetic field model GRIMM_L120 (version 0.0) and the main magnetic field model of 10 IGRF11. The corresponding results at the poles are discussed and the validity of the derived formulas is verified using the Laplace equation of the potential field.

1 Introduction

Compared to the magnetic vector and scalar measurements, magnetic gradients lead 15 to more robust models of the lithospheric magnetic field. The ongoing ESA's *Swarm* mission, will provide measurements not only of the vector and scalar data but also an estimate of their east–west gradients (e.g. Olsen et al., 2004; Friis-Christensen et al., 2006). Kotsiaros and Olsen (2012, 2014) proposed to recover the lithospheric magnetic field through Magnetic Space Gradiometry in the same way that has been done for modeling the gravitational potential field from the GOCE satellite gravity gradient tensor measurements. Purucker et al. (2005, 2007) also reported efforts to model 20 the lithospheric magnetic field using magnetic gradient information from the Ørsted, CHAMP, SAC-C and ST-5 constellation. Their results showed that by using gradients data, the modelled lithospheric magnetic anomaly field has enhanced shorter wavelength content and has a much higher quality compared to models built from vector field data. This is because the gradients data can remove the highly time-dependant

Non-singular spherical harmonic expressions of geomagnetic fields

J. Du et al.

[Title Page](#)

[Abstract](#)

[Introduction](#)

[Conclusions](#)

[References](#)

[Tables](#)

[Figures](#)

◀

▶

◀

▶

[Back](#)

[Close](#)

[Full Screen / Esc](#)

[Printer-friendly Version](#)

[Interactive Discussion](#)



contributions of the magnetosphere and ionosphere that are correlated between two side-by-side satellites.

The order-2 magnetic gradient tensor consists of spatial derivatives highlighting certain structures of the magnetic field (e.g. Schmidt and Clark, 2000, 2006). It can be used to detect the hidden and small-scale magnetized sources (e.g. Pedersen and Rasmussen, 1990; Harrison and Southam, 1991) and to investigate the orientation of the lineated magnetic anomalies (e.g. Blakely and Simpson, 1986). Quantitative magnetic interpretation methods such as the analytic signal, edge detection, spatial derivatives, Euler deconvolution, and transforms, all set in Cartesian coordinate system (e.g. Blakely, 1995; Purucker and Whaler, 2007; Taylor et al., 2014) also require calculating the higher-order derivatives of the magnetic anomaly field and need to be extended to regional and global scales to handle the curvature of the Earth and other planets. Ravat et al. (2002) and Ravat (2011) utilized the analytic signal method and the total gradient to interpret the satellite-altitude magnetic anomaly data. Therefore, both the magnetic field modelling and also the geological interpretations require the calculation for the partial derivatives of the magnetic field in form of spherical harmonics, possibly at the poles for specific systems of coordinates. Spherical harmonic analysis (SHA), established originally by Gauss (1839), is generally used to model the global magnetic lithospheric field of the Earth and other terrestrial planets (e.g. Maus et al., 2008; Langlais et al., 2009; Thébault et al., 2010; Lesur et al., 2013; Sabaka et al., 2013; Olsen et al., 2014). Series of spherical harmonic functions themselves made of Schmidt semi-normalized associated Legendre functions (SSALFs) (e.g. Blakely, 1995; Langel and Hinze, 1998), are fitted by least-squares to magnetic measurements, giving the spherical harmonic coefficients i.e. the Gaussian coefficients defining the model. Kotsiaros and Olsen (2012, 2014) presented the MV and the MGT using a spherical harmonic representation and, of course, their expressions are singular as they approach the poles. Even if there are satellite data gaps around the poles, it is advisable to use non-singular spherical harmonic expressions for the MV and the MGT in case

Non-singular spherical harmonic expressions of geomagnetic fields

J. Du et al.

[Title Page](#)

[Abstract](#)

[Introduction](#)

[Conclusions](#)

[References](#)

[Tables](#)

[Figures](#)

◀

▶

◀

▶

[Back](#)

[Close](#)

[Full Screen / Esc](#)

[Printer-friendly Version](#)

[Interactive Discussion](#)



airborne or shipborne magnetic data are utilized (e.g. Golynsky et al., 2013; Maus, 2010).

In this paper, following Petrovskaya and Vershkov (2006) and Eshagh (2008, 2009) for the gravitational gradient tensor in the local-north-oriented reference frame (LNORF), the non-singular expressions in terms of spherical harmonics for the MV, the MGT and the higher-order derivatives of the magnetic anomaly field in the LNORF are presented. In the next section, the traditional expressions of the MV and the MGT are first stated, then some necessary propositions are proved and at last new non-singular expressions are derived. In Sect. 3, the new formulae are tested using the global lithospheric magnetic field model GRIMM_L120 (version 0.0) (Lesur et al., 2013) and the main magnetic field model of IGRF11 (Finlay et al., 2010). Finally, further applications 10 are discussed and some conclusions are also drawn.

2 Methodology

In this section, the traditional expressions of MV and MGT are presented, and their numerical problems are stated. Then based on the mathematical derivations, new expressions are given.

2.1 Traditional expressions

The scalar potential V of the Earth's magnetic field in a source-free region can be expanded in the truncated series of spherical harmonics at the point $P(r, \theta, \varphi)$ (e.g. Backus et al., 1996):

$$V(r, \theta, \varphi) = a \sum_{l=1}^L \sum_{m=0}^l \left(\frac{a}{r}\right)^{l+1} (g_l^m \cos m\varphi + h_l^m \sin m\varphi) \tilde{P}_l^m(\cos \theta), \quad (1)$$

where $a = 6371.2$ km is the radius of the Earth's magnetic reference sphere; r , θ and φ are geocentric radius, co-latitude and longitude, respectively; $\tilde{P}_l^m(\cos \theta)$ (or \tilde{P}_l^m for

[Title Page](#)

[Abstract](#)

[Introduction](#)

[Conclusions](#)

[References](#)

[Tables](#)

[Figures](#)

◀

▶

◀

▶

[Back](#)

[Close](#)

[Full Screen / Esc](#)

[Printer-friendly Version](#)

[Interactive Discussion](#)



simplification) is the SSALF of degree l and order m ; L is the maximum spherical harmonic degree; g_l^m and h_l^m are the geomagnetic harmonic coefficients describing internal sources of the Earth.

If considered in the LNORF \mathbf{x}_P , \mathbf{y}_P , \mathbf{z}_P at the point $P(r, \varphi, \theta)$, where \mathbf{z}_P axis points downward in geocentric radial direction, \mathbf{x}_P axis points to the north, and \mathbf{y}_P axis towards the east (that is, a right-handed system). At the poles, we define that \mathbf{y}_P axis points to the meridian of 90° E. Therefore, the three components of the MV can be expressed as:

$$\begin{aligned} B_x(r, \theta, \varphi) &= -\frac{1}{r} \frac{\partial}{\partial(-\theta)} V(r, \theta, \varphi) \\ &= \sum_{l=1}^L \sum_{m=0}^l \left(\frac{a}{r}\right)^{l+2} (g_l^m \cos m\varphi + h_l^m \sin m\varphi) \left[\frac{\partial}{\partial\theta} \tilde{P}_l^m(\cos\theta) \right], \end{aligned} \quad (2a)$$

$$\begin{aligned} B_y(r, \theta, \varphi) &= -\frac{1}{r \sin\theta} \frac{\partial}{\partial\varphi} V(r, \theta, \varphi) \\ &= \sum_{l=1}^L \sum_{m=0}^l \left(\frac{a}{r}\right)^{l+2} m(g_l^m \sin m\varphi - h_l^m \cos m\varphi) \left[\frac{1}{\sin\theta} \tilde{P}_l^m(\cos\theta) \right], \end{aligned} \quad (2b)$$

$$\begin{aligned} B_z(r, \theta, \varphi) &= -\frac{\partial}{\partial(-r)} V(r, \theta, \varphi) \\ &= -\sum_{l=1}^L \sum_{m=0}^l (l+1) \left(\frac{a}{r}\right)^{l+2} (g_l^m \cos m\varphi + h_l^m \sin m\varphi) \tilde{P}_l^m(\cos\theta). \end{aligned} \quad (2c)$$

The MGT can be written as (e.g. Kotsiaros and Olsen, 2012)

$$\nabla \mathbf{B} = \begin{pmatrix} B_{xx} & B_{xy} & B_{xz} \\ B_{yx} & B_{yy} & B_{yz} \\ B_{zx} & B_{zy} & B_{zz} \end{pmatrix} = \begin{pmatrix} \partial B_x / \partial x & \partial B_x / \partial y & \partial B_x / \partial z \\ \partial B_y / \partial x & \partial B_y / \partial y & \partial B_y / \partial z \\ \partial B_z / \partial x & \partial B_z / \partial y & \partial B_z / \partial z \end{pmatrix}, \quad (3)$$

Title Page

Abstract

Introduction

Conclusions

References

Tables

Figures

◀

▶

◀

▶

Back

Close

Full Screen / Esc

Printer-friendly Version

Interactive Discussion

Non-singular spherical harmonic expressions of geomagnetic fields

J. Du et al.

[Title Page](#)

[Abstract](#)

[Introduction](#)

[Conclusions](#)

[References](#)

[Tables](#)

[Figures](#)

◀

▶

◀

▶

[Back](#)

[Close](#)

[Full Screen / Esc](#)

[Printer-friendly Version](#)

[Interactive Discussion](#)



where nine elements are expressed respectively as:

$$B_{xx} = \frac{1}{a} \sum_{l=1}^L \sum_{m=0}^l \left(\frac{a}{r}\right)^{l+3} (g_l^m \cos m\varphi + h_l^m \sin m\varphi) \times \left[-\frac{\partial^2}{\partial\theta^2} \tilde{P}_l^m(\cos\theta) + (l+1) \tilde{P}_l^m(\cos\theta) \right], \quad (4a)$$

$$B_{xy} = B_{yx} = \frac{1}{a} \sum_{l=1}^L \sum_{m=0}^l \left(\frac{a}{r}\right)^{l+3} m (g_l^m \sin m\varphi - h_l^m \cos m\varphi) \times \left[-\frac{1}{\sin\theta} \frac{\partial}{\partial\theta} \tilde{P}_l^m(\cos\theta) + \frac{\cos\theta}{\sin^2\theta} \tilde{P}_l^m(\cos\theta) \right], \quad (4b)$$

$$B_{xz} = B_{zx} = \frac{1}{a} \sum_{l=1}^L \sum_{m=0}^l \left(\frac{a}{r}\right)^{l+3} (l+2) (g_l^m \cos m\varphi + h_l^m \sin m\varphi) \left[\frac{\partial}{\partial\theta} \tilde{P}_l^m(\cos\theta) \right], \quad (4c)$$

$$B_{yy} = \frac{1}{a} \sum_{l=1}^L \sum_{m=0}^l \left(\frac{a}{r}\right)^{l+3} (g_l^m \cos m\varphi + h_l^m \sin m\varphi) \times \left[(l+1) \tilde{P}_l^m(\cos\theta) + \frac{m^2}{\sin^2\theta} \tilde{P}_l^m(\cos\theta) - \frac{\cos\theta}{\sin\theta} \frac{\partial}{\partial\theta} \tilde{P}_l^m(\cos\theta) \right], \quad (4d)$$

$$B_{yz} = B_{zy} = \frac{1}{a} \sum_{l=1}^L \sum_{m=0}^l \left(\frac{a}{r}\right)^{l+3} (l+2)m (g_l^m \sin m\varphi - h_l^m \cos m\varphi) \left[\frac{1}{\sin\theta} \tilde{P}_l^m(\cos\theta) \right], \quad (4e)$$

$$B_{zz} = -\frac{1}{a} \sum_{l=1}^L \sum_{m=0}^l \left(\frac{a}{r}\right)^{l+3} (l+1)(l+2) (g_l^m \cos m\varphi + h_l^m \sin m\varphi) \tilde{P}_l^m(\cos\theta). \quad (4f)$$

The expressions for B_z and B_{zz} can be calculated stably even for very high SH degrees and orders by using the Holmes and Featherstone (2002a) scheme. However,

[Title Page](#)[Abstract](#)[Introduction](#)[Conclusions](#)[References](#)[Tables](#)[Figures](#)[◀](#)[▶](#)[◀](#)[▶](#)[Back](#)[Close](#)[Full Screen / Esc](#)[Printer-friendly Version](#)[Interactive Discussion](#)

there exist the singular terms of $1/\sin\theta$ and $1/\sin^2\theta$ in Eqs. (2b), (4b), (4d) and (4e) when the computing point approaches to the poles. Besides, some expressions contain the terms of first- and second-order derivatives of SSALFs, such as Eqs. (2a) and (4a)–(4d). Nevertheless, the second-order derivative for very high degree and orders of SSALFs can be recursively calculated by the Clenshaw or Horner algorithms (Holmes and Featherstone, 2002b). These algorithms are relatively complicated and thus we want to use alternative expressions to avoid the singular terms and the partial derivatives of SSALFs.

2.2 Mathematical derivations

- To deal with the singular terms and first- and second-order derivatives of the SSALFs, some useful mathematical derivations are introduced and proved in the following.

1 – Derivation of $\partial\tilde{P}_l^m/\partial\theta$

Based on the Eq. (Z.1.44) in Ilk (1983)

$$\partial P_l^m / \partial \theta = 0.5 [(l+m)(l-m+1) P_l^{m-1} - P_l^{m+1}], \quad (5)$$

- and the relation between the ALFs and the SSALFs as

$$\tilde{P}_l^m = \sqrt{C_m(l-m)!/(l+m)!} P_l^m, \quad (6)$$

thus the first-order derivative of the SSALFs can be deduced as:

$$\partial \tilde{P}_l^m / \partial \theta = a_{l,m} \tilde{P}_l^{m-1} + b_{l,m} \tilde{P}_l^{m+1}, \quad (7a)$$

$$a_{l,m} = 0.5 \sqrt{l+m} \sqrt{l-m+1} \sqrt{C_m/C_{m-1}}, \quad (7b)$$

$$b_{l,m} = -0.5 \sqrt{l+m+1} \sqrt{l-m} \sqrt{C_m/C_{m+1}}, \quad (7c)$$

where $C_m = 2 - \delta_{m,0} = \begin{cases} 1, & m=0 \\ 2, & m \neq 0 \end{cases}$ and δ is the Kronecker's delta function.

2 – Derivation of $\partial^2 \tilde{P}_l^m / \partial \theta^2$

According to the Eq. (23) in Eshagh (2008) as

$$\begin{aligned} \partial^2 P_l^m / \partial \theta^2 &= 0.25(l+m)(l-m+1)(l+m-1)(l-m+2)P_l^{m-2} \\ &\quad - 0.25[(l+m)(l-m+1) + (l-m)(l+m+1)]P_l^m + 0.25P_l^{m+2}, \end{aligned} \quad (8)$$

5

the second-order derivative of the SSALFs can be written as:

$$\partial^2 \tilde{P}_l^m / \partial \theta^2 = c_{l,m} \tilde{P}_l^{m-2} + d_{l,m} \tilde{P}_l^m + e_{l,m} \tilde{P}_l^{m+2}, \quad (9a)$$

$$c_{l,m} = 0.25 \sqrt{l+m} \sqrt{l+m-1} \sqrt{l-m+2} \sqrt{l-m+1} \sqrt{C_m/C_{m-2}}, \quad (9b)$$

$$d_{l,m} = -0.25[(l+m)(l-m+1) + (l-m)(l+m+1)], \quad (9c)$$

$$e_{l,m} = 0.25 \sqrt{l+m+2} \sqrt{l+m+1} \sqrt{l-m} \sqrt{l-m-1} \sqrt{C_m/C_{m+2}}. \quad (9d)$$

3 – Derivation of $\tilde{P}_l^m / \sin \theta$

Using the Eq. (Z.1.42) in Ilk (1983)

$$P_l^m / \sin \theta = 0.5[(l+m)(l+m-1)P_{l-1}^{m-1} + P_{l-1}^{m+1}] / m, \quad m \geq 1, \quad (10)$$

and the Eq. (6), we can obtain that

$$\tilde{P}_l^m / \sin \theta = f_{l,m} \tilde{P}_{l-1}^{m-1} + g_{l,m} \tilde{P}_{l-1}^{m+1}, \quad m \geq 1, \quad (11a)$$

$$f_{l,m} = 0.5 \sqrt{l+m} \sqrt{l+m-1} \sqrt{C_m/C_{m-1}} / m, \quad m \geq 1, \quad (11b)$$

$$g_{l,m} = 0.5 \sqrt{l-m} \sqrt{l-m-1} \sqrt{C_m/C_{m+1}} / m, \quad m \geq 1. \quad (11c)$$

Non-singular spherical harmonic expressions of geomagnetic fields

J. Du et al.

[Title Page](#)

[Abstract](#)

[Introduction](#)

[Conclusions](#)

[References](#)

[Tables](#)

[Figures](#)

◀

▶

◀

▶

[Back](#)

[Close](#)

[Full Screen / Esc](#)

[Printer-friendly Version](#)

[Interactive Discussion](#)



4 – Derivation of $\tilde{P}_l^m / \sin^2 \theta$

Employing the Eq. (31) in Eshagh (2008) as

$$\begin{aligned} P_l^m / \sin^2 \theta &= \{(l+m)(l+m-1)(l-m+1)(l-m+2)/(m-1)P_l^{m-2} \\ &\quad + [(l+m)(l+m-1)/(m-1) + (l-m)(l-m-1)/(m+1)]P_l^m \\ &\quad + 1/(m+1)P_l^{m+2}\}/(4m), \quad m \geq 2, \end{aligned} \quad (12)$$

5

and the Eq. (6), we have

$$\tilde{P}_l^m / \sin^2 \theta = h_{l,m} \tilde{P}_l^{m-2} + k_{l,m} \tilde{P}_l^m + n_{l,m} \tilde{P}_l^{m+2}, \quad m \geq 2, \quad (13a)$$

$$h_{l,m} = 0.25 \sqrt{l+m} \sqrt{l+m-1} \sqrt{l-m+1} \sqrt{l-m+2} \sqrt{C_m/C_{m-2}} / [m(m-1)], \quad m \geq 2, \quad (13b)$$

$$k_{l,m} = 0.25 [(l+m)(l+m-1)/(m-1) + (l-m)(l-m-1)/(m+1)]/m, \quad m \geq 2, \quad (13c)$$

$$n_{l,m} = 0.25 \sqrt{l-m} \sqrt{l-m-1} \sqrt{l+m+2} \sqrt{l+m+1} \sqrt{C_m/C_{m+2}} / [m(m+1)], \quad m \geq 1. \quad (13d)$$

5 – Derivation of $\partial \tilde{P}_l^m / (\sin \theta \partial \theta)$

Using the Eq. (36) in Eshagh (2008) as

$$\begin{aligned} \partial P_l^m / (\sin \theta \partial \theta) &= 0.25 \{(l+m)(l+m-1)(l+m-2)(l-m+1)/(m-1)P_{l-1}^{m-2} \\ &\quad + [(l+m)(l-m+1)/(m-1) - (l+m+1)(l+m)/(m+1)]P_l^m \\ &\quad - 1/(m+1)P_{l-1}^{m+2}\}, \quad m \geq 2, \end{aligned} \quad (14)$$

15

J. Du et al.

[Title Page](#)[Abstract](#)[Introduction](#)[Conclusions](#)[References](#)[Tables](#)[Figures](#)[◀](#)[▶](#)[◀](#)[▶](#)[Back](#)[Close](#)[Full Screen / Esc](#)[Printer-friendly Version](#)[Interactive Discussion](#)

[Title Page](#)[Abstract](#)[Introduction](#)[Conclusions](#)[References](#)[Tables](#)[Figures](#)[|](#)[|](#)[◀](#)[▶](#)[Back](#)[Close](#)[Full Screen / Esc](#)[Printer-friendly Version](#)[Interactive Discussion](#)

and the Eq. (6), we can derive

$$\partial \tilde{P}_l^m / (\sin \theta \partial \theta) = o_{l,m} \tilde{P}_{l-1}^{m-2} + q_{l,m} \tilde{P}_{l-1}^m + x_{l,m} \tilde{P}_{l-1}^{m+2}, \quad m \geq 2, \quad (15a)$$

$$o_{l,m} = 0.25 \sqrt{l+m} \sqrt{l+m-1} \sqrt{l+m-2} \sqrt{l-m+1} \sqrt{C_m/C_{m-2}} / (m-1), \quad m \geq 2, \quad (15b)$$

$$q_{l,m} = 0.25 \sqrt{l-m} \sqrt{l+m} [(l-m+1)/(m-1) - (l+m+1)/(m+1)], \quad m \geq 2, \quad (15c)$$

$$x_{l,m} = -0.25 \sqrt{l+m+1} \sqrt{l-m} \sqrt{l-m-1} \sqrt{l-m-2} \sqrt{C_m/C_{m+2}} / (m+1). \quad (15d)$$

6 – Derivation of $\partial \tilde{P}_l^m / (\sin \theta \partial \theta) - \tilde{P}_l^m \cos \theta / \sin^2 \theta$

According to Petrovskaya and Vershkov (2006) and Eshagh (2009), we can write

$$\begin{aligned} \partial P_l^m / (\sin \theta \partial \theta) - P_l^m \cos \theta / \sin^2 \theta &= \\ 0.5 [(m-1)(l+m)(l-m+1)P_l^{m-1} / \sin \theta - (m+1)P_l^{m+1} / \sin \theta] / m, \quad m \geq 1, \end{aligned} \quad (16)$$

and using the Eq. (36) in Eshagh (2008), we can obtain

$$P_l^{m-1} / \sin \theta = 0.5 [(l-m+2)(l-m+3)P_{l+1}^{m-2} + P_{l+1}^m] / (m-1), \quad m \geq 2, \quad (17a)$$

$$P_l^{m+1} / \sin \theta = 0.5 [(l-m)(l-m+1)P_{l+1}^m + P_{l+1}^{m+2}] / (m+1). \quad (17b)$$

Substituting the Eq. (17) into the right hand side of the Eq. (16) and after simplification, we can derive

$$\begin{aligned} \partial P_l^m / (\sin \theta \partial \theta) - P_l^m \cos \theta / \sin^2 \theta &= 0.25 [(l+m)(l-m+1)(l-m+2)(l-m+3)P_{l+1}^{m-2} \\ &+ 2m(l-m+1)P_{l+1}^m - P_{l+1}^{m+2}] / m, \quad m \geq 1. \end{aligned} \quad (18)$$

[Title Page](#)[Abstract](#)[Introduction](#)[Conclusions](#)[References](#)[Tables](#)[Figures](#)[|◀](#)[▶|](#)[◀](#)[▶](#)[Back](#)[Close](#)[Full Screen / Esc](#)[Printer-friendly Version](#)[Interactive Discussion](#)

And combining the Eq. (6), we obtain that

$$\begin{aligned} \partial \tilde{P}_l^m / (\sin \theta \partial \theta) - \tilde{P}_l^m \cos \theta / \sin^2 \theta = \\ 0.25 & \left[\sqrt{l+m} \sqrt{l-m+1} \sqrt{l-m+2} \sqrt{l-m+3} \sqrt{C_m/C_{m-2}} \tilde{P}_{l+1}^{m-2} \right. \\ & + 2m \sqrt{l-m+1} \sqrt{l+m+1} \tilde{P}_{l+1}^m \\ & \left. - \sqrt{l+m+1} \sqrt{l+m+2} \sqrt{l+m+3} \sqrt{l-m} \sqrt{C_m/C_{m+2}} \tilde{P}_{l+1}^{m+2} \right] / m, \quad m \geq 1. \end{aligned} \quad (19)$$

7 – Derivation of $[(l+1)\sin^2 \theta \tilde{P}_l^m + m^2 \tilde{P}_l^m - \sin \theta \cos \theta \partial \tilde{P}_l^m / \partial \theta] / \sin^2 \theta$

Based on the Lemma 3 in Eshagh (2009) as

$$\sin \theta \cos \theta \partial P_l^m / \partial \theta = m P_l^m + (l+1) \sin^2 \theta P_l^m - \sin \theta P_{l+1}^{m+1}, \quad (20)$$

we can derive

$$\begin{aligned} [(l+1)\sin^2 \theta P_l^m + m^2 P_l^m - \sin \theta \cos \theta \partial P_l^m / \partial \theta] / \sin^2 \theta = \\ m(m-1) P_l^m / \sin^2 \theta + P_{l+1}^{m+1} / \sin \theta. \end{aligned} \quad (21)$$

According to the Eq. (10), we can write

$$P_{l+1}^{m+1} / \sin \theta = 0.5 [(l+m+2)(l+m+1) P_l^m + P_l^{m+2}] / (m+1). \quad (22)$$

Inserting the Eqs. (12) and (22) into the Eq. (21), and after some simplifications, we obtain that

$$\begin{aligned} [(l+1)\sin^2 \theta P_l^m + m^2 P_l^m - \sin \theta \cos \theta \partial P_l^m / \partial \theta] / \sin^2 \theta = \\ 0.25(l+m)(l+m-1)(l-m+1)(l-m+2) P_l^{m-2} \\ + 0.25 [(l+m)(l+m-1) + (l-m)(l-m-1)(m-1) / (m+1) \\ + 2(l+m+2)(l+m+1) / (m+1)] P_l^m + 0.25 P_l^{m+2}. \end{aligned} \quad (23)$$

And combining with the Eq. (6), we can derive

$$\begin{aligned}
 & [(l+1)\sin^2\theta \tilde{P}_l^m + m^2 \tilde{P}_l^m - \sin\theta \cos\theta \partial \tilde{P}_l^m / \partial\theta] / \sin^2\theta = \\
 & 0.25 \sqrt{l+m} \sqrt{l+m-1} \sqrt{l-m+1} \sqrt{l-m+2} \sqrt{C_m/C_{m-2}} \tilde{P}_l^{m-2} \\
 & + 0.25 [(l+m)(l+m-1) + (l-m)(l-m-1)(m-1)/(m+1) \\
 & + 2(l+m+2)(l+m+1)/(m+1)] \tilde{P}_l^m \\
 & + 0.25 \sqrt{l+m+1} \sqrt{l+m+2} \sqrt{l-m} \sqrt{l-m-1} \sqrt{C_m/C_{m+2}} \tilde{P}_l^{m+2}. \tag{24}
 \end{aligned}$$

2.3 New expressions

Inserting the corresponding mathematical derivations in the last section into the Eqs. (2) and (4) and after some simplifications, the new expressions for the MV and the MGT can be written as:

$$B_x = \sum_{l=1}^L \sum_{m=0}^l \left(\frac{a}{r}\right)^{l+2} (g_l^m \cos m\varphi + h_l^m \sin m\varphi) (a_{l,m}^x \tilde{P}_l^{m-1} + b_{l,m}^x \tilde{P}_l^{m+1}), \tag{25a}$$

$$B_y = \sum_{l=1}^L \sum_{m=0}^l \left(\frac{a}{r}\right)^{l+2} (g_l^m \sin m\varphi - h_l^m \cos m\varphi) (a_{l,m}^y \tilde{P}_{l-1}^{m-1} + b_{l,m}^y \tilde{P}_{l-1}^{m+1}), \tag{25b}$$

$$B_z = \sum_{l=1}^L \sum_{m=0}^l \left(\frac{a}{r}\right)^{l+2} (g_l^m \cos m\varphi + h_l^m \sin m\varphi) (a_{l,m}^z \tilde{P}_l^m), \tag{25c}$$

$$B_{xx} = \frac{1}{a} \sum_{l=1}^L \sum_{m=0}^l \left(\frac{a}{r}\right)^{l+3} (g_l^m \cos m\varphi + h_l^m \sin m\varphi) (a_{l,m}^{xx} \tilde{P}_l^{m-2} + b_{l,m}^{xx} \tilde{P}_l^m + c_{l,m}^{xx} \tilde{P}_l^{m+2}), \tag{26a}$$

Title Page	Abstract	Introduction
Conclusions	References	
Tables	Figures	
◀	▶	
◀	▶	
Back	Close	
Full Screen / Esc		
Printer-friendly Version		
Interactive Discussion		



$$B_{xy} = \frac{1}{a} \sum_{l=1}^L \sum_{m=0}^l \left(\frac{a}{r}\right)^{l+3} (g_l^m \sin m\varphi - h_l^m \cos m\varphi) \left(a_{l,m}^{xy} \tilde{P}_{l+1}^{m-2} + b_{l,m}^{xy} \tilde{P}_l^m + c_{l,m}^{xy} \tilde{P}_{l+1}^{m+2} \right), \quad (26b)$$

$$B_{xz} = \frac{1}{a} \sum_{l=1}^L \sum_{m=0}^l \left(\frac{a}{r}\right)^{l+3} (g_l^m \cos m\varphi + h_l^m \sin m\varphi) \left(a_{l,m}^{xz} \tilde{P}_l^{m-1} + b_{l,m}^{xz} \tilde{P}_l^{m+1} \right), \quad (26c)$$

$$B_{yy} = \frac{1}{a} \sum_{l=1}^L \sum_{m=0}^l \left(\frac{a}{r}\right)^{l+3} (g_l^m \cos m\varphi + h_l^m \sin m\varphi) \left(a_{l,m}^{yy} \tilde{P}_l^{m-2} + b_{l,m}^{yy} \tilde{P}_l^m + c_{l,m}^{yy} \tilde{P}_l^{m+2} \right), \quad (26d)$$

$$B_{yz} = \frac{1}{a} \sum_{l=1}^L \sum_{m=0}^l \left(\frac{a}{r}\right)^{l+3} (g_l^m \sin m\varphi - h_l^m \cos m\varphi) \left(a_{l,m}^{yz} \tilde{P}_{l-1}^{m-1} + b_{l,m}^{yz} \tilde{P}_{l-1}^{m+1} \right), \quad (26e)$$

$$B_{zz} = \frac{1}{a} \sum_{l=1}^L \sum_{m=0}^l \left(\frac{a}{r}\right)^{l+3} (g_l^m \cos m\lambda + h_l^m \sin m\varphi) a_{l,m}^{zz} \tilde{P}_l^m. \quad (26f)$$

Furthermore, some other higher-order partial derivatives and their transforms are usually used to image geologic boundaries in magnetic prospecting (e.g. Hsu et al., 1996). Therefore, we also give the third-order partial derivatives of the spherical harmonics as following:

$$\begin{aligned} B_{xxz} &= \frac{\partial B_{xx}}{\partial z} = \frac{\partial^2 B_x}{\partial x \partial z} = \frac{\partial^2 B_x}{\partial z \partial x} \\ &= \frac{1}{a^2} \sum_{l=1}^L \sum_{m=0}^l \left(\frac{a}{r}\right)^{l+4} (g_l^m \cos m\varphi + h_l^m \sin m\varphi) \left(a_{l,m}^{xxz} \tilde{P}_l^{m-2} + b_{l,m}^{xxz} \tilde{P}_l^m + c_{l,m}^{xxz} \tilde{P}_l^{m+2} \right), \end{aligned} \quad (27a)$$

$$B_{xyz} = \frac{\partial B_{xy}}{\partial z} = \frac{\partial B_{yx}}{\partial z} = \frac{\partial^2 B_x}{\partial y \partial z} = \frac{\partial^2 B_x}{\partial z \partial y} = \frac{\partial^2 B_y}{\partial x \partial z} = \frac{\partial^2 B_y}{\partial z \partial x}$$

Non-singular spherical harmonic expressions of geomagnetic fields

J. Du et al.

[Title Page](#)

[Abstract](#)

[Introduction](#)

[Conclusions](#)

[References](#)

[Tables](#)

[Figures](#)

◀

▶

◀

▶

[Back](#)

[Close](#)

[Full Screen / Esc](#)

[Printer-friendly Version](#)

[Interactive Discussion](#)



$$= \frac{1}{a^2} \sum_{l=1}^L \sum_{m=0}^l \left(\frac{a}{r}\right)^{l+4} (g_l^m \sin m\varphi - h_l^m \cos m\varphi) (a_{l,m}^{xyz} \tilde{P}_{l+1}^{m-2} + b_{l,m}^{xyz} \tilde{P}_{l+1}^m + c_{l,m}^{xyz} \tilde{P}_{l+1}^{m+2}), \quad (27b)$$

$$\begin{aligned} B_{xzz} &= \frac{\partial B_{xz}}{\partial z} = \frac{\partial B_{zx}}{\partial z} = \frac{\partial^2 B_x}{\partial z^2} = \frac{\partial^2 B_z}{\partial x \partial z} = \frac{\partial^2 B_z}{\partial z \partial x} \\ &= \frac{1}{a^2} \sum_{l=1}^L \sum_{m=0}^l \left(\frac{a}{r}\right)^{l+4} (g_l^m \cos m\varphi + h_l^m \sin m\varphi) (a_{l,m}^{xzz} \tilde{P}_l^{m-1} + b_{l,m}^{xzz} \tilde{P}_l^{m+1}), \end{aligned} \quad (27c)$$

$$\begin{aligned} B_{yyz} &= \frac{\partial B_{yy}}{\partial z} = \frac{\partial^2 B_y}{\partial y \partial z} = \frac{\partial^2 B_y}{\partial z \partial y} \\ &= \frac{1}{a^2} \sum_{l=1}^L \sum_{m=0}^l \left(\frac{a}{r}\right)^{l+4} (g_l^m \cos m\varphi + h_l^m \sin m\varphi) (a_{l,m}^{yyz} \tilde{P}_l^{m-2} + b_{l,m}^{yyz} \tilde{P}_l^m + c_{l,m}^{yyz} \tilde{P}_l^{m+2}), \end{aligned} \quad (27d)$$

$$\begin{aligned} B_{yzz} &= \frac{\partial B_{yz}}{\partial z} = \frac{\partial B_{zy}}{\partial z} = \frac{\partial^2 B_y}{\partial z^2} = \frac{\partial^2 B_z}{\partial y \partial z} = \frac{\partial^2 B_z}{\partial z \partial y} \\ &= \frac{1}{a^2} \sum_{l=1}^L \sum_{m=0}^l \left(\frac{a}{r}\right)^{l+4} (g_l^m \sin m\lambda - h_l^m \cos m\lambda) (a_{l,m}^{yzz} \tilde{P}_{l-1}^{m-1} + b_{l,m}^{yzz} \tilde{P}_{l-1}^{m+1}), \end{aligned} \quad (27e)$$

$$\begin{aligned} B_{zzz} &= \frac{\partial^2 B_z}{\partial z^2} \\ &= \frac{1}{a^2} \sum_{l=1}^L \sum_{m=0}^l \left(\frac{a}{r}\right)^{l+4} (g_l^m \cos m\varphi + h_l^m \sin m\varphi) a_{l,m}^{zzz} \tilde{P}_l^m, \end{aligned} \quad (27f)$$

- where the corresponding coefficients of the SSALFs are presented in Appendix A and can be computed once for all points. In this way, we avoid computing recursively the

J. Du et al.

[Title Page](#)

[Abstract](#)

[Introduction](#)

[Conclusions](#)

[References](#)

[Tables](#)

[Figures](#)

◀

▶

◀

▶

[Back](#)

[Close](#)

[Full Screen / Esc](#)

[Printer-friendly Version](#)

[Interactive Discussion](#)



Non-singular spherical harmonic expressions of geomagnetic fields

J. Du et al.

[Title Page](#)

[Abstract](#)

[Introduction](#)

[Conclusions](#)

[References](#)

[Tables](#)

[Figures](#)

◀

▶

◀

▶

[Back](#)

[Close](#)

[Full Screen / Esc](#)

[Printer-friendly Version](#)

[Interactive Discussion](#)



SSALFs, their first- and second-order derivatives respectively with the traditional formulae. These new relations do not suffer from the singular terms and don't contain the derivatives. The cost is only to calculate two additional degrees and orders for the SSALFs at most. In this study, we use the conventional form of SSALF that if $m < 0$, then $\tilde{P}_l^m = (-1)^{|m|} \tilde{P}_l^{|m|}$ and if $m > l$, then $\tilde{P}_l^m = 0$.

3 Numerical investigation

We test the derived expressions and the numerical implementation in C/C++, by calculating the magnetic potential, vector and its gradients on a grid with $0.125^\circ \times 0.125^\circ$ cell size at the altitude of 300 km relative to the Earth's magnetic reference sphere using the magnetic field models defined by: (i) the lithospheric magnetic field model GRIMM_L120 (version 0.0) (Lesur et al., 2013); (ii) the main magnetic field model IGRF11 (Finlay et al., 2010) at the epoch of 2005.0.0. The global magnetic potential V , the MV and the MGT mapped by the lithospheric field and the main field are shown in Figs. 1 and 2, respectively. The corresponding statistics are presented in Tables 1 and 2. A simple test is that the MGT meets the Laplace's equation of the potential field, that is, the trace of the MGT should be equal to zero. Our numerical results show that the amplitude of $B_{xx} + B_{yy} + B_{zz}$ is in the range of $[-8.0 \times 10^{-14} \text{ pT m}^{-1} / +8.0 \times 10^{-14} \text{ pT m}^{-1}]$ ($1 \text{ pT m}^{-1} = 10^{-3} \text{ nT m}^{-1} = 1 \text{ nT km}^{-1}$). The relative error is almost equal the machine accuracy. Therefore, this feature proves the validity of our derived formulae. In addition, as shown in Fig. 1, it is obvious that the MGT enhances the lineation and contacts. It also reveals some small-scale anomalies, which is very helpful for the further geological interpretation. Figure 2 illustrates that the gradients of the main field are very smooth but the amplitudes are still very high. Furthermore, the computed magnetic fields are smooth near the poles and don't have the singularities at the poles as shown in Fig. 3. The magnetic potential V , B_z and B_{zz} components at the poles are independent of the direction of the x_P and y_P axes. How-

ever, while changing with the direction of the x_P and y_P axes at the poles, the B_x , B_y , B_{xz} , B_{yz} components have a period of 360° and the B_{xx} , B_{xy} and B_{yy} components have a period of 180° . Therefore, at the poles we specially define that the x_P axis points to the meridian of 180° E (or 180° W) at north pole and 0° E at south pole and the y_P axis points to the meridian of 90° E, that is, the LNORF moving from Greenwich meridian to the poles.

4 Discussion and conclusions

We develop in this paper the new expressions for the MV, the MGT and the third-order partial derivatives of the magnetic field in terms of spherical harmonics. The traditional expressions have complicated forms involving first- and second-order derivatives of the SSALFs and are singular when approaching to the poles. Our newly derived formulae don't contain the first- and second-order derivatives of the SSALFs and remove the singularities at the poles.

However, our formulae are derived in the spherical local north-oriented reference frame with specific definition at the poles. For an application to the magnetic data of a satellite gradiometry mission, it is necessary to describe the MV and the MGT in the local orbital reference frame, where the new MV and MGT are the linear functions of the MV and the new MGT in the LNORF with coefficients related to the satellite track azimuth (e.g. Petrovskaya and Vershkov, 2006). The other main purpose of this paper is in the future to contribute to the signal processing and the geological interpretation of lithospheric magnetic field model, especially in polar areas.

[Title Page](#)[Abstract](#)[Introduction](#)[Conclusions](#)[References](#)[Tables](#)[Figures](#)[◀](#)[▶](#)[◀](#)[▶](#)[Back](#)[Close](#)[Full Screen / Esc](#)[Printer-friendly Version](#)[Interactive Discussion](#)

Appendix A: Additional formulae

Numerical constants in the Eqs. (25)–(27) are expressed in following:

$$\begin{cases} a_{l,m}^x = 0.5\sqrt{l+m}\sqrt{l-m+1}\sqrt{C_m/C_{m-1}} \\ b_{l,m}^x = -0.5\sqrt{l+m+1}\sqrt{l-m}\sqrt{C_m/C_{m+1}}, \end{cases} \quad (A1)$$

$$\begin{cases} a_{l,m}^y = 0.5\sqrt{l+m}\sqrt{l+m-1}\sqrt{C_m/C_{m-1}} \\ b_{l,m}^y = 0.5\sqrt{l-m}\sqrt{l-m-1}\sqrt{C_m/C_{m+1}}, \end{cases} \quad (A2)$$

$$a_{l,m}^z = -(l+1), \quad (A3)$$

$$\begin{cases} a_{l,m}^{xx} = -0.25\sqrt{l+m}\sqrt{l+m-1}\sqrt{l-m+2}\sqrt{l-m+1}\sqrt{C_m/C_{m-2}} \\ b_{l,m}^{xx} = 0.25[(l+m)(l-m+1)+(l-m)(l+m+1)]+(l+1) \\ c_{l,m}^{xx} = -0.25\sqrt{l+m+2}\sqrt{l+m+1}\sqrt{l-m}\sqrt{l-m-1}\sqrt{C_m/C_{m+2}}, \end{cases} \quad (A4)$$

$$\begin{cases} a_{l,m}^{xy} = -0.25\sqrt{l+m}\sqrt{l-m+1}\sqrt{l-m+2}\sqrt{l-m+3}\sqrt{C_m/C_{m-2}} \\ b_{l,m}^{xy} = -0.5m\sqrt{l-m+1}\sqrt{l+m+1} \\ c_{l,m}^{xy} = 0.25\sqrt{l+m+1}\sqrt{l+m+2}\sqrt{l+m+3}\sqrt{l-m}\sqrt{C_m/C_{m+2}}, \end{cases} \quad (A5)$$

$$\begin{cases} a_{l,m}^{xz} = 0.5(l+2)\sqrt{l+m}\sqrt{l-m+1}\sqrt{C_m/C_{m-1}} = (l+2)a_{l,m}^x \\ b_{l,m}^{xz} = -0.5(l+2)\sqrt{l+m+1}\sqrt{l-m}\sqrt{C_m/C_{m+1}} = (l+2)b_{l,m}^x, \end{cases} \quad (A6)$$

$$\begin{cases} a_{l,m}^{yy} = 0.25\sqrt{l+m}\sqrt{l+m-1}\sqrt{l-m+1}\sqrt{l-m+2}\sqrt{C_m/C_{m-2}} \\ b_{l,m}^{yy} = 0.25[(l+m)(l+m-1)+(l-m)(l-m-1)(m-1)/(m+1) \\ + 2(l+m+2)(l+m+1)/(m+1)] \\ c_{l,m}^{yy} = 0.25\sqrt{l+m+1}\sqrt{l+m+2}\sqrt{l-m}\sqrt{l-m-1}\sqrt{C_m/C_{m+2}}, \end{cases} \quad (A7)$$

[Title Page](#)

[Abstract](#)

[Introduction](#)

[Conclusions](#)

[References](#)

[Tables](#)

[Figures](#)

◀

▶

◀

▶

[Back](#)

[Close](#)

[Full Screen / Esc](#)

[Printer-friendly Version](#)

[Interactive Discussion](#)



$$\begin{cases} a_{l,m}^{yz} = 0.5(l+2)\sqrt{l+m}\sqrt{l+m-1}\sqrt{C_m/C_{m-1}} = (l+2)a_{l,m}^y \\ b_{l,m}^{yz} = 0.5(l+2)\sqrt{l-m}\sqrt{l-m-1}\sqrt{C_m/C_{m+1}} = (l+2)b_{l,m}^y, \end{cases} \quad (A8)$$

$$a_{l,m}^{zz} = -(l+1)(l+2) = (l+2)a_{l,m}^z, \quad (A9)$$

$$\begin{cases} a_{l,m}^{xxz} = (l+3)a_{l,m}^{xx} \\ b_{l,m}^{xxz} = (l+3)b_{l,m}^{xx} \\ c_{l,m}^{xxz} = (l+3)c_{l,m}^{xx}, \end{cases} \quad (A10)$$

$$\begin{cases} a_{l,m}^{xyz} = (l+3)a_{l,m}^{xy} \\ b_{l,m}^{xyz} = (l+3)b_{l,m}^{xy} \\ c_{l,m}^{xyz} = (l+3)c_{l,m}^{xy}, \end{cases} \quad (A11)$$

$$\begin{cases} a_{l,m}^{xzz} = 0.5(l+2)(l+3)\sqrt{l+m}\sqrt{l-m+1}\sqrt{C_m/C_{m-1}} \\ \quad = (l+2)(l+3)a_{l,m}^x = (l+3)a_{l,m}^{xz} \\ b_{l,m}^{xzz} = -0.5(l+2)(l+3)\sqrt{l+m+1}\sqrt{l-m}\sqrt{C_m/C_{m+1}} \\ \quad = (l+2)(l+3)b_{l,m}^x = (l+3)b_{l,m}^{xz}, \end{cases} \quad (A12)$$

$$\begin{cases} a_{l,m}^{yyz} = (l+3)a_{l,m}^{yy} \\ b_{l,m}^{yyz} = (l+3)b_{l,m}^{yy} \\ c_{l,m}^{yyz} = (l+3)c_{l,m}^{yy}, \end{cases} \quad (A13)$$

$$\begin{cases} a_{l,m}^{yzz} = 0.5(l+2)(l+3)\sqrt{l+m}\sqrt{l+m-1}\sqrt{C_m/C_{m-1}} \\ \quad = (l+2)(l+3)a_{l,m}^y = (l+3)a_{l,m}^{yz} \\ b_{l,m}^{yzz} = 0.5(l+2)(l+3)\sqrt{l-m}\sqrt{l-m-1}\sqrt{C_m/C_{m+1}} \\ \quad = (l+2)(l+3)b_{l,m}^y = (l+3)b_{l,m}^{yz}, \end{cases} \quad (A14)$$

Non-singular spherical harmonic expressions of geomagnetic fields

J. Du et al.

[Title Page](#)

[Abstract](#)

[Introduction](#)

[Conclusions](#)

[References](#)

[Tables](#)

[Figures](#)

◀

▶

◀

▶

[Back](#)

[Close](#)

[Full Screen / Esc](#)

[Printer-friendly Version](#)

[Interactive Discussion](#)



$$a_{l,m}^{zzz} = -(l+1)(l+2)(l+3) = (l+3)a_{l,m}^{zz} = (l+2)(l+3)a_{l,m}^z. \quad (\text{A15})$$

Code availability

Supplementary software implementation is performed by the programming language C/C++. The source code and input data presented in this paper can be obtained
5 by contacting the corresponding author via email or download from the Supplement related to the online version of this article.

**The Supplement related to this article is available online at
doi:10.5194/gmdd-7-8477-2014-supplement.**

Acknowledgements. This study is supported by International Cooperation Projection in
10 Science and Technology (No.: 2010DFA24580). Jinsong Du is sponsored by the China Scholarship Council (CSC). We would like to thank Mehdi Eshagh for his fruitful discussions. All projected figures are drawn using the Generic Mapping Tools (GMT) (Wessel and Smith, 1991).

15 The service charges for this open access publication have been covered by a Research Centre of the Helmholtz Association.

References

- Backus, G. E., Parker, R., and Constable, C.: Foundations of Geomagnetism, Cambridge University Press, Cambridge, 1996.
- 20 Bird, P.: An updated digital model of plate boundaries, *Geochem. Geophys. Geosy.*, 4, 1027, doi:10.1029/2001GC000252, 2003.
- Blakely, R. G.: Potential Theory in Gravity and Magnetic Applications, Cambridge University Press, New York, 1995.
- 25 Blakely, R. J. and Simpson, R. W.: Approximating edges of source bodies from magnetic or gravity anomalies, *Geophysics*, 51, 1494–1498, 1986.
- Eshagh, M.: Non-singular expressions for the vector and gradient tensor of gravitation in a geocentric spherical frame, *Comput. Geosci.*, 34, 1762–1768, 2008.

[Title Page](#)

[Abstract](#)

[Introduction](#)

[Conclusions](#)

[References](#)

[Tables](#)

[Figures](#)

◀

▶

◀

▶

[Back](#)

[Close](#)

[Full Screen / Esc](#)

[Printer-friendly Version](#)

[Interactive Discussion](#)



- Eshagh, M.: Alternative expressions for gravity gradients in local north-oriented frame and tensor spherical harmonics, *Acta Geophys.*, 58, 215–243, 2009.
- Finlay, C. C., Maus, S., Beggan, C. D., Bondar, T. N., Chambodut, A., Chernova, T. A., Chulliat, A., Golovkov, V. P., Hamilton, B., Hamoudi, M., Holme, R., Hulot, G., Kuang, W.,
5 Langlais, B., Lesur, V., Lowes, F. J., Lühr, H., Macmillan, S., Mandea, M., McLean, S., Manoj, C., Menville, M., Michaelis, I., Olsen, N., Rauberg, J., Rother, M., Sabaka, T. J., Tangborn, A., Tøffner-Clausen, L., Thébault, E., Thomson, A. W. P., Wardinski, I., Wei, Z., and Zvereva, T. I.: International geomagnetic reference field: the eleventh generation, *Geophys. J. Int.*, 183, 1216–1230, 2010.
- 10 Friis-Christensen, E., Lühr, H., and Hulot, G.: Swarm: a constellation to study the Earth's magnetic field, *Earth Planets Space*, 58, 351–358, 2006.
- Gauss, C. F.: Allgemeine Theorie des Erdmagnetismus, in: Resultate aus den Beobachtungen
des magnetischen Vereins im Jahre 1838, edited by: Gauss, C. F. and Weber, W., Weidmannsche Buchhandlung, Leipzig, 1839, 1–57, 1838.
- 15 Golynsky, A., Bell, R., Blankenship, D., Damaske, D., Ferraccioli, F., Finn, C., Golynsky, D., Ivanov, S., Jokat, W., Masolov, V., Riedel, S., von Frese, R., Young, D., and ADMAP Working Group: Air and shipborne magnetic surveys of the Antarctic into the 21st century, *Tectono-physics*, 585, 3–12, 2013.
- Harrison, C. and Southam, J.: Magnetic field gradients and their uses in the study of the Earth's
20 magnetic field, *J. Geomagn. Geoelectr.*, 43, 485–599, 1991.
- Holmes, S. A. and Featherstone, W. E.: A unified approach to the Clenshaw summation and
the recursive computation of very high degree and order normalized associated Legendre
functions, *J. Geodesy*, 76, 279–299, 2002a.
- 25 Holmes, S. A. and Featherstone, W. E.: SHORT NOTES: extending simplified high-degree syn-
thesis methods to second latitudinal derivatives of geopotential, *J. Geodesy*, 76, 447–450,
2002b.
- Hsu, S. K., Sibuet, J. C., and Shyu, C. T.: High-resolution detection of geologic boundaries from
potential-field anomalies: an enhanced analytic signal technique, *Geophysics*, 61, 373–386,
1996.
- 30 Ilk, K. H.: Ein Beitrag zur Dynamik ausgedehnter Körper – Gravitationswechselwirkung, Reihe
C, Heft Nr. 288, Deutsche Geodätische Kommission, München, 1983.
- Kotsiaros, S. and Olsen, N.: The geomagnetic field gradient tensor: properties and parametriza-
tion in terms of spherical harmonics, *Int. J. Geomath.*, 3, 297–314, 2012.

J. Du et al.

[Title Page](#)[Abstract](#)[Introduction](#)[Conclusions](#)[References](#)[Tables](#)[Figures](#)[◀](#)[▶](#)[◀](#)[▶](#)[Back](#)[Close](#)[Full Screen / Esc](#)[Printer-friendly Version](#)[Interactive Discussion](#)

- Kotsiaros, S. and Olsen, N.: End-to-End simulation study of a full magnetic gradiometry mission, *Geophys. J. Int.*, 196, 100–110, 2014.
- Langel, R. A. and Hinze, W. J.: *The Magnetic Field of the Earth's Lithosphere: the Satellite Perspective*, Cambridge University Press, Cambridge, UK, 1998.
- 5 Langlais, B., Lesur, V., Purucker, M. E., Connerney, J. E. P., and Mandea, M.: Crustal magnetic fields of terrestrial planets, *Space Sci. Rev.*, 152, 223–249, 2010.
- Lesur, V., Rother, M., Vervelidou, F., Hamoudi, M., and Thébault, E.: Post-processing scheme for modelling the lithospheric magnetic field, *Solid Earth*, 4, 105–118, doi:10.5194/se-4-105-2013, 2013.
- 10 Maus, S.: An ellipsoidal harmonic representation of Earth's lithospheric magnetic field to degree and order 720, *Geochem. Geophys. Geosy.*, 11, Q06015, doi:10.1029/2010GC003026, 2010.
- Maus, S., Yin, F., Lühr, H., Manoj, C., Rother, M., Rauberg, J., Michaelis, I., Stolle, C., and Müller, R. D.: Resolution of direction of oceanic magnetic lineations by the sixth-generation lithospheric magnetic field model from CHAMP satellite magnetic measurements, *Geochem. Geophys. Geosy.*, 9, Q07021, doi:10.1029/2008GC001949, 2008.
- 15 Olsen, N. and the Swarm End-to-End Consortium: Swarm-End-to-End mission performance simulator study, ESA contract No. 17263/02/NL/CB, DSRI Report 1/2004, Danish Space Research Institute, Copenhagen, 2004.
- Olsen, N., Lühr, H., Finlay, C. C., Sabaka, T. J., Michaelis, I., Rauberg, J., and Tøffner-Clausen, L.: The CHAOS-4 geomagnetic field model, *Geophys. J. Int.*, 197, 815–827, 2014.
- Pedersen, L. B. and Rasmussen, T. M.: The gradient tensor of potential field anomalies: some implications on data collection and data processing of maps, *Geophysics*, 55, 1558–1566, 2000.
- Petrovskaya, M. S. and Vershkov, A. N.: Non-singular expressions for the gravity gradients in the local north-oriented and orbital reference frames, *J. Geodesy*, 80, 117–127, 2006.
- 25 Purucker, M. E.: Lithospheric studies using gradients from close encounters of Ørsted, CHAMP and SAC-C, *Earth Planets Space*, 57, 1–7, 2005.
- Purucker, M. and Whaler, K.: Crustal magnetism, in: *Treatise on Geophysics*, vol. 5, *Geomagnetism*, edited by: Kono, M., Elsevier, Amsterdam, 195–237, 2007.
- 30 Purucker, M., Sabaka, T., Le, G., Slavin, J. A., Strangeway, R. J., and Busby, C.: Magnetic field gradients from the ST-5 constellation: improving magnetic and thermal models of the lithosphere, *Geophys. Res. Lett.*, 34, L24306, doi:10.1029/2007GL031739, 2007.

Non-singular spherical harmonic expressions of geomagnetic fields

J. Du et al.

[Title Page](#)

[Abstract](#)

[Introduction](#)

[Conclusions](#)

[References](#)

[Tables](#)

[Figures](#)

◀

▶

◀

▶

[Back](#)

[Close](#)

[Full Screen / Esc](#)

[Printer-friendly Version](#)

[Interactive Discussion](#)



**Non-singular
spherical harmonic
expressions of
geomagnetic fields**

J. Du et al.

- Ravat, D.: Interpretation of Mars southern highlands high amplitude magnetic field with total gradient and fractal source modeling: new insights into the magnetic mystery of Mars, *Icarus*, 214, 400–412, 2011.
- Ravat, D., Wang, B., Wildermuth, E., and Taylor, P. T.: Gradients in the interpretation of satellite-altitude magnetic data: an example from central Africa, *J. Geodyn.*, 33, 131–142, 2002.
- Sabaka, T. J., Tøffner-Claussen, L., and Olsen, N.: Use of the comprehensive inversion method for swarm satellite data analysis, *Earth Planets Space*, 65, 1201–1222, 2013.
- Schmidt, P. and Clark, D.: Advantages of measuring the magnetic gradient tensor, *Preview*, 85, 26–30, 2000.
- Schmidt, P. and Clark, D.: The magnetic gradient tensor: its properties and uses in source characterization, *The Leading Edge*, 25, 75–78, 2006.
- Taylor, P. T., Kis, K. I., and Wittmann, G.: Satellite-altitude horizontal magnetic gradient anomalies used to define the Kursk magnetic anomaly, *J. Appl. Geophys.*, 109, 133–139, doi:10.1016/j.jappgeo.2014.07.018, 2014.
- Thébault, E., Purucker, M., Whaler, K. A., Langlais, B., and Sabaka, T. J.: The magnetic field of Earth's lithosphere, *Space Sci. Rev.*, 155, 95–127, 2010.
- Wessel, P. and Smith, W. H. F.: Free software helps map and display data, *EOS Trans. AGU*, 72, 441–446, 1991.

Discussion Paper | Discussion Paper

[Title Page](#)[Abstract](#)[Introduction](#)[Conclusions](#)[References](#)[Tables](#)[Figures](#)[◀](#)[▶](#)[◀](#)[▶](#)[Back](#)[Close](#)[Full Screen / Esc](#)[Printer-friendly Version](#)[Interactive Discussion](#)

Non-singular spherical harmonic expressions of geomagnetic fields

J. Du et al.

Table 1. Statistics of the global magnetic potential V , the MV and the MGT at the altitude of 300 km using the lithospheric magnetic field model GRIMM_L120 (version 0.0) (Lesur et al., 2013) for spherical harmonic degrees 16 ~ 90.

	Min.	Max.	Mean	SD
V [T × m]	-0.006977	+0.007065	+0.000025	+0.001202
B_x [nT]	-31.404860	+19.957069	+0.022759	+3.442116
B_y [nT]	-27.602360	+21.606852	-0.000014	+3.164313
B_z [nT]	-37.626160	+42.107562	-0.075795	+4.670772
B_{xx} [pT m ⁻¹]	-0.128025	+0.157735	+0.000014	+0.015455
B_{xy} [pT m ⁻¹]	-0.081758	+0.072777	+1.562 × 10 ⁻⁸	+0.007914
B_{xz} [pT m ⁻¹]	-0.203059	+0.140263	+0.000377	+0.017661
B_{yy} [pT m ⁻¹]	-0.178822	+0.099738	+0.000238	+0.013513
B_{yz} [pT m ⁻¹]	-0.188019	+0.180890	-3.390 × 10 ⁻⁷	+0.015838
B_{zz} [pT m ⁻¹]	-0.249113	+0.302516	-0.000252	+0.024152
$B_{xx} + B_{yy} + B_{zz}$ [pT m ⁻¹]	-2.050 × 10 ⁻¹⁵	+2.026 × 10 ⁻¹⁵	+2.641 × 10 ⁻¹⁹	+5.062 × 10 ⁻¹⁶

Non-singular spherical harmonic expressions of geomagnetic fields

J. Du et al.

Table 2. Statistics of the global magnetic potential V , the MV and the MGT at the altitude of 300 km using the main magnetic field model IGRF11 (Finlay et al., 2011) at the epoch of 2005.0.0 for spherical harmonic degrees 1 ~ 13.

	Min.	Max.	Mean	SD
V [T × m]	−173.724200	+179.405770	−2.546835	+121.548200
B_x [nT]	−13 606.960000	+35 541.860000	+15 770.336000	+9989.476700
B_y [nT]	−14 041.740000	+13 606.962000	+1.631590	+5446.330400
B_z [nT]	−57 345.060000	+52 129.744000	+922.317400	+36 357.077000
B_{xx} [pT m ^{−1}]	−13.028350	+14.578552	−0.137809	+8.535842
B_{xy} [pT m ^{−1}]	−1.660599	+1.995721	−0.000102	+0.807332
B_{xz} [pT m ^{−1}]	−8.457901	+18.331623	+6.917859	+5.214859
B_{yy} [pT m ^{−1}]	−12.967040	+13.720839	−0.238961	+7.968691
B_{yz} [pT m ^{−1}]	−9.161899	+8.457901	+0.000759	+3.264648
B_{zz} [pT m ^{−1}]	−28.022720	+25.865197	+0.376770	+16.432027
$B_{xx} + B_{yy} + B_{zz}$ [pT m ^{−1}]	-7.460×10^{-14}	$+7.816 \times 10^{-14}$	-4.580×10^{-17}	$+1.033 \times 10^{-14}$

Non-singular spherical harmonic expressions of geomagnetic fields

J. Du et al.

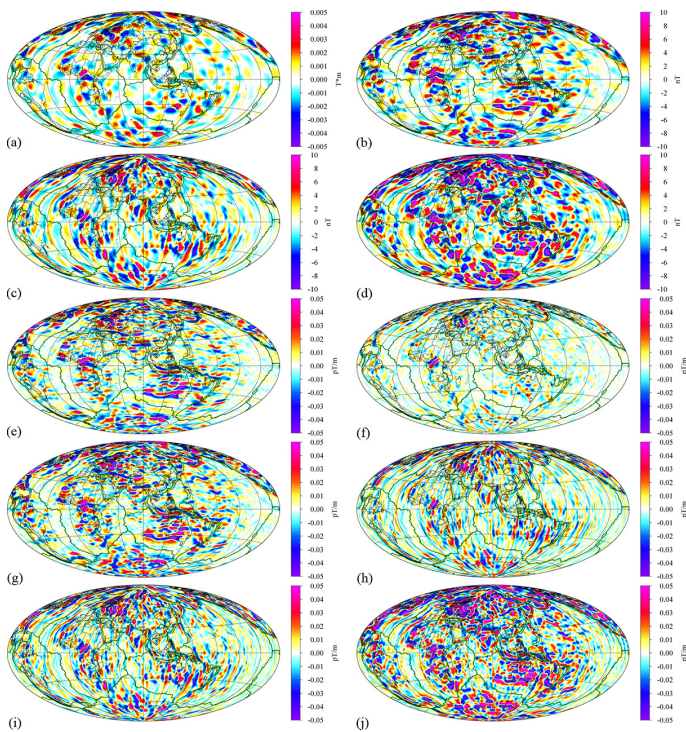


Figure 1. Global lithospheric magnetic potential, vector and its gradients fields at the altitude of 300 km as defined by the lithospheric magnetic field model GRIMM_L120 (version 0.0) (Lesur et al., 2013) for spherical harmonic degrees 16 ~ 90. **(a)** is magnetic potential (V), **(b-d)** are three components (B_x , B_y and B_z) of magnetic vector, **(e-j)** are six elements (B_{xx} , B_{xy} , B_{xz} , B_{yy} , B_{yz} and B_{zz}) of magnetic gradient tensor, respectively. The dark green lines are the plate boundaries by Bird (2003). All maps are shown on a Hammer projection centered at 90° E.

[Title Page](#)

[Abstract](#)

[Introduction](#)

[Conclusions](#)

[References](#)

[Tables](#)

[Figures](#)

◀

▶

◀

▶

[Back](#)

[Close](#)

[Full Screen / Esc](#)

[Printer-friendly Version](#)

[Interactive Discussion](#)

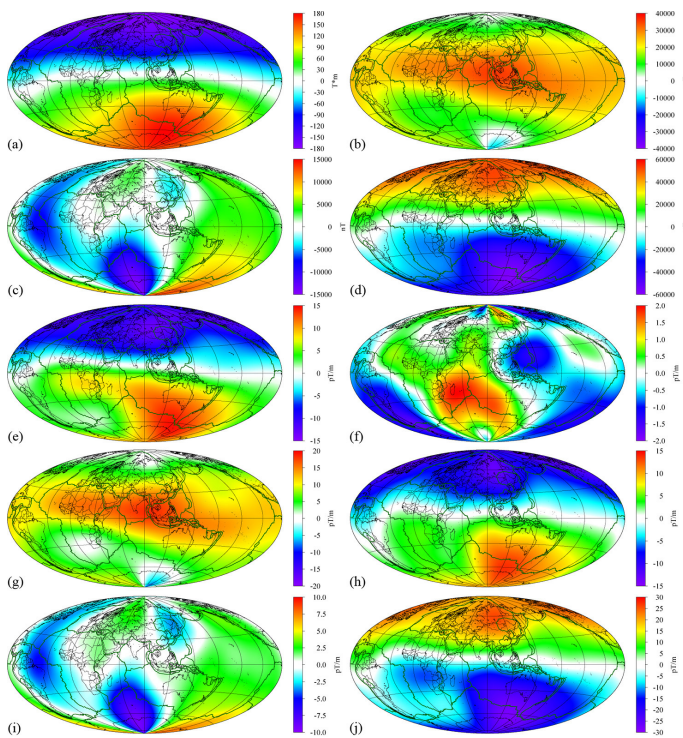


Figure 2. Global magnetic potential, vector and its gradients fields of the main field at the altitude of 300 km as defined by the main magnetic field model IGRF11 (Finlay et al., 2011) at the epoch of 2005.0.0 for spherical harmonic degrees 1 ~ 13. **(a)** is magnetic potential (V), **(b-d)** are three components (B_x , B_y and B_z) of magnetic vector, **(e-j)** are six elements (B_{xx} , B_{xy} , B_{xz} , B_{yy} , B_{yz} and B_{zz}) of magnetic gradient tensor, respectively. The dark green lines are the plate boundaries by Bird (2003). All maps are shown on a Hammer projection centered at 90° E.

Non-singular spherical harmonic expressions of geomagnetic fields

J. Du et al.

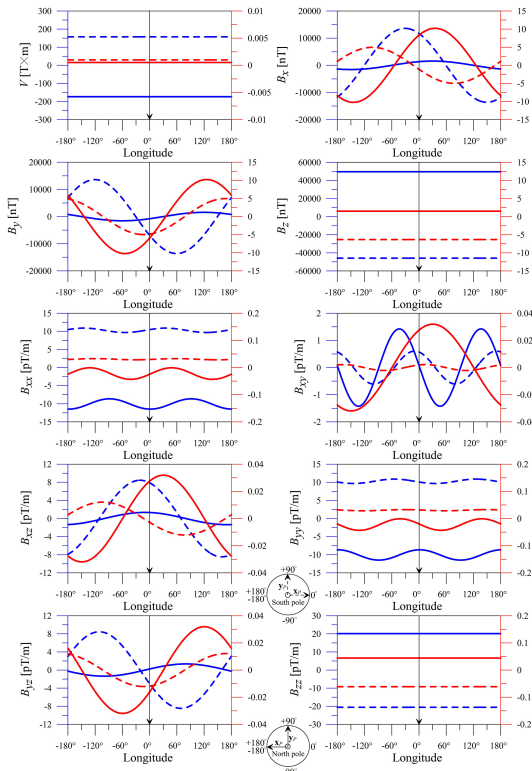


Figure 3. Limit values of magnetic potential (V), vector (B_x , B_y and B_z) and its gradients (B_{xx} , B_{xy} , B_{xz} , B_{yy} , B_{yz} and B_{zz}) at the poles when the local reference frames vary from different meridians (the direction of x_P axe changing from different meridian to the poles). Solid and dashed lines indicate the magnetic effects at north-pole and at south-pole, respectively. Red and blue lines indicate the lithosphere the x_P axis points to the meridian of 180° E (or 180° W) at north pole and 0° E at south pole and the y_P axis points to the meridian of 90° E.

Title Page

Abstract

Introduction

Conclusions

References

Tables

Figures

◀

▶

◀

▶

Back

Close

Full Screen / Esc

Printer-friendly Version

Interactive Discussion